

Meteorology

Impacts of the ocean-atmosphere coupling into the very short range prediction system, during the impact of Hurricane Matthew on Cuba

Impacto do acoplamento oceano-atmosfera no sistema de previsão de muito curto prazo, durante o impacto do furacão Matthew em Cuba

Liset Vázquez Proveyer^I , Maibys Sierra Lorenzo^I ,
Roberto Carlos Cruz Rodríguez^{II} , John C Warner^{III} 

^I Cuban Institute of Meteorology, Havana, Cuba

^{II} National Autonomous University of Mexico, DF, Mexico

^{III} Woods Hole Coastal and Marine Science Center, Woods Hole, MA, United States

ABSTRACT

The main goal of this investigation is analyzing the impact of insert the ocean-atmosphere coupling into the very short range prediction system of Cuba. The ocean-atmosphere coupled components of the Coupled Ocean-Atmosphere-Wave-Sediment Transport Modeling System are used for this purpose and the hurricane Matthew is selected as study case. Two experiments are performed: first, using a dynamic sea surface temperature, updated daily in the atmospheric model WRF; and second using a dynamic coupling between the atmospheric and an oceanic models. For the simulated track, the best results are obtained with the coupled system. The impact of coupling on the maximum wind velocities and minimum central pressure is studied. In the coupled system the sea surface temperature has more influence in the surface latent heat fluxes. Also, with this methodology the dry footprint and the behavior of the precipitation field in the presence of a hurricane are studied. This analysis shows that the hurricane acts like an open and self-sustained system in the numerical experiments. The highest differences in the precipitation simulations are in the significant convective area inside the hurricane.

Keywords: Atmospheric dynamics; Sea surface temperature; Hurricane Matthew; Coupled ocean-atmosphere modeling system; Very short range prediction system

RESUMO

O objetivo principal desta investigação é analisar o impacto da inserção do acoplamento oceano-atmosfera no sistema de previsão de muito curto prazo de Cuba. Os componentes acoplados oceano-atmosfera do Sistema de Modelagem Acoplado Oceano-Atmosfera-Onda-Transporte do Sedimento, são usados para este propósito e o furacão Matthew é selecionado como caso de estudo. Dois experimentos são realizados: primeiro, usando uma temperatura dinâmica da superfície do mar atualizada diariamente o WRF; e a segunda usando um acoplamento dinâmico entre os modelos atmosférico e oceânico. Para a trajetória simulada, os melhores resultados são obtidos com o sistema acoplado. O impacto do acoplamento nas velocidades máximas do vento e na pressão central mínima é estudado. No sistema acoplado, a temperatura da superfície do mar tem mais influência nos fluxos de calor latente à superfície. Além disso, com esta metodologia a pegada seca e o comportamento do campo de precipitação na presença de um furacão são estudados. Esta análise mostra que o furacão atua como um sistema aberto e autossustentável nos experimentos numéricos. As maiores diferenças nas simulações de precipitação estão na significativa área convectiva dentro do furacão.

Palavras-chave: Dinâmica atmosférica; Temperatura da superfície do mar; Furacão Matthew; Sistema de modelagem oceano-atmosfera acoplado; Sistema de previsão de muito curto prazo

1 INTRODUCTION

Due to the insular features of Cuba, and its narrow and elongated configuration, the weather conditions are mainly determined from the Caribbean Sea state. For this reason, in the weather forecast, it is necessary to consider the ocean-atmosphere interaction. Also, in presence of extreme phenomena like tropical cyclones, the knowledge of sea conditions plays a fundamental role in the prediction accuracy of those systems such as, in the reduction and prediction of disasters associated with strong winds, heavy rain and sea swells, fundamentally at the seashores Warner *et al.* (2010), Hegermiller *et al.* (2019). Also, it is shown that the effect of the ocean-hurricane interaction produced a significant cooling of the sea surface; and the decrease in the sea surface temperature is the primary mechanism affecting the storm intensity caused by the ocean interaction Bender e Ginis (2000).

At present, in Cuba, forecasters use the Very Short Term Prediction System (SisPI by its acronym in Spanish) Sierra-Lorenzo *et al.* (2014), Sierra-Lorenzo *et al.* (2017) based in the atmospheric model Weather Research and Forecast (WRF) Michalakes *et al.* (2005). Although SisPI uses a dynamic SST Vázquez-Proveyer *et al.* (2017), it can be

improved with the implementation of coupled ocean-atmosphere models. These numerical systems allow a better representation of the physical processes such as interaction at the sea-air interface Warner *et al.* (2010), Zambon *et al.* (2014).

The main goal of this investigation is to evaluate the incorporation of the ocean-atmosphere coupling in the SisPI. For this, sensitivity studies and experiments using the coupled ocean-atmosphere module of the Coupled Ocean-Atmosphere-WaveSediment Transport (COAWST) Modeling System Warner *et al.* (2010), Warner *et al.* (2019) are carried out. The hurricane Matthew case is selected to analyze the SisPI's behavior in representing the influence of the sea surface temperature in the atmospheric dynamics.

Studies in the coastal region around Cuba have focused on improving the numerical forecast of oceanic variables, using forecast output fields of atmospheric models Mitrani-Arenal *et al.* (2019). This work shows a dynamic coupled method between oceanic and atmospheric numerical components, which allows improving both, atmospheric and oceanic forecasts, being the first investigation of that topic in this region.

This article is organized as follows. In section 2, a brief description of the COAWST modeling system and the experiments is given. The principal results obtained in the simulations are shown in section 3 by comparing our experiments with a combination of verification data. Finally, the conclusions of this investigation are presented.

2 MATERIALS AND METHODS

In this section, first, an introduction to the COAWST Modeling System is given and the case study is presented. Later, the experiments design and the verification data are described.

2.1 COAWST

The Coupled Ocean-Atmosphere-Wave-Sediment Transport Modeling System is a set of open-source modeling components that had been combined to study coupled processes of atmosphere, ocean, wave and sediments transport in coastal ocean Warner *et al.* (2010). The Model Coupling Toolkit (MCT) Larson *et al.* (2001) is used as a coupler to exchange data fields between: the Regional Oceanic Modeling System (ROMS) Shchepetkin e McWilliams (2005), the WRF, the Simulating Wave Nearshore (SWAN) Booij *et al.* (1997) and the sediments capabilities of Community Sediment Transport Model (CSTM) Geyer *et al.* (2007). The system also includes a method for regridding (Warner *et al.* (2010), Warner *et al.* (2019)). In this work, only the coupled ocean-atmosphere components are used.

2.2 Hurricane Matthew, the case study

Since 2012, the 2016 hurricane season was the first with above-average cyclonic activity. Hurricane Matthew was the most intense and deadliest hurricane of that season, and also the one that caused more material damage in our region. It caused 585 direct deaths in Haiti, the United States of America, the Dominican Republic and Saint Vincent and the Grenadines. The material damages, reported by the affected countries, are estimated at USD 10.6 billion Ballester e Rubiera (2016).

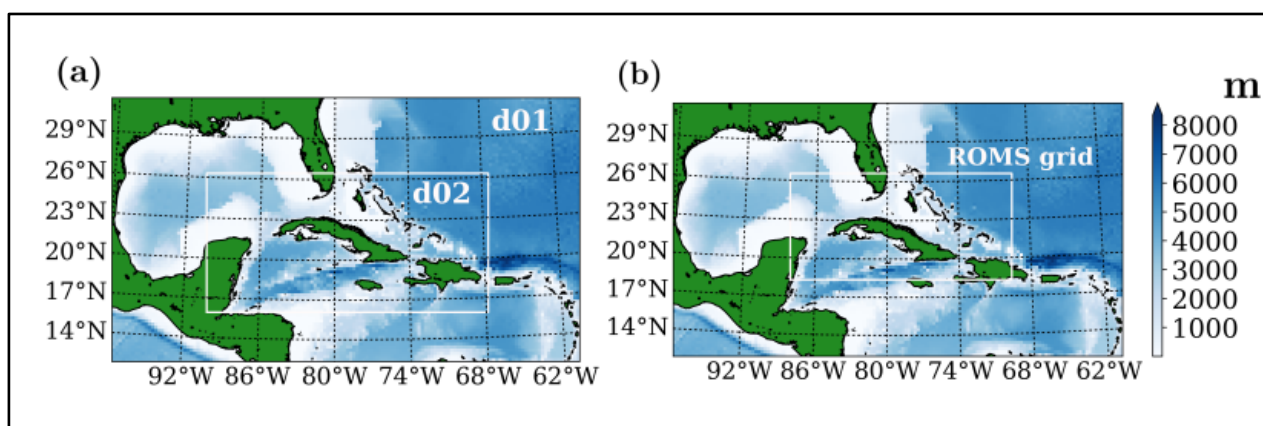
Matthew was the only hurricane that directly affected Cuba during the 2016 hurricane season. No deaths, but great material damages were caused. Strong winds, precipitation, swells and coastal flooding on the eastern Cuban coast were the principal effects of the hurricane Ballester e Rubiera (2016).

2.3 Experiment design

The simulation period is from October 4th (0000 UTC) to October 7th (0000 UTC) when the hurricane Matthew directly affected Cuba, realizing a 72-hour forecast. To

evaluate the SisPI performance when a coupled ocean-atmosphere module is used, two numerical experiments are performed. First using the original SisPI configuration that uses a dynamic sea surface temperature in the WRF model (WRF (SST)), which consists of a daily updated SST in the atmospheric model and second, using a dynamic coupling between ROMS and WRF models, with the MCT (WRF-ROMS).

Image 1 - Representation of the bathymetry field (in meters) in the studied area (a) WRF nested domains of 27 km (d01) and 9 km (d02). (b) ROMS domain



Source: created by the author (PROVEYER, 2021)

2.3.1 Atmospheric model configuration

The COAWST atmospheric component adopts the SisPI configuration Sierra-Lorenzo *et al.* (2014), Sierra-Lorenzo *et al.* (2017) with some modifications:

1. Initialization is done with the Global Forecast System (GFS) forecast and SST data of 0.5 using 26 vertical levels.
2. Nested domains of 27 and 9 km resolution (Figure 1(a)).
3. Lambert Conformal Conic projection
4. Domains centering in 22.30 N and 79.1 W, approximately center of Cuba
5. Time step: 150 seconds.
6. Parameterization of microphysics: WRF Single-Moment Microphysics Scheme (WSM5) Lim *et al.* (2004).
7. Parameterization of cumulus: Grell-Freitas Grell e Freitas (2014).

The dynamic SST is obtained from a daily, high-resolution, real-time, global, sea surface temperature (RTG_SST_HR) analysis, that has been developed at the National Centers for Environmental Prediction/Marine Modeling and Analysis Branch (NCEP/MMAB). The RTG_SST_HR product is produced on a half-degree (latitude, longitude) grid, with a two-dimensional variational interpolation analysis of the most recent 24-hours buoy and ship data, satellite-retrieved SST data, and SST's derived from satellite-observed sea-ice coverage (Gemmill *et al.*, 2007).

2.3.2 Oceanic model configuration

The grid for the ROMS model is obtained from the parent domain of the WRF model (27 km), with a spatial resolution of 9 km (Figure 1(b)) and land-mask interpolated data. The main features of the oceanic model configuration are:

1. Initialization with Hybrid Coordinate Ocean Model (HYCOM) data of 8 km of resolution Wallcraft *et al.* (2003).
2. 12 vertical levels
3. Lambert Conformal Conic projection
4. Domain centering in 22.30 N and 79.1 W, approximately center of Cuba
5. Time step: 15 seconds.
6. Vertical layer transformation equation: $V_{transform} = 2$
7. Vertical stretching function: $V_{stretching} = 4$

To improve the land-mask, shore lines are obtained from the Global Self-consistent, Hierarchical, High-resolution Geography Database (GSHHG) Wessel e Smith (1996). The tide data used are obtained from the global model TPXO7 with a spatial resolution of 0.25 Egbert e Erofeeva (2002) and the GFS data is used to initialize the dynamic forcing in the oceanic model. The bathymetry data are obtained from an update of the General Bathymetric Chart of the Ocean (GEBCO) published in 2014. Bathymetry and elevation data contained in GEBCO are distributed in a 30 arcseconds, global mesh Weatherall *et al.* (2015).

2.3.3 Regridding and coupling

Because the atmospheric and oceanic domains have different resolution, interpolation is needed to allow the data exchange between components. For that reason, the Spherical Coordinate Remapping Interpolation Package (SCRIP) Jones (1999) is used to calculate the interpolation weights, which are calculated during the preprocessing and read as a matrix in the model initialization. In the synchronization points, these weights are used to transform the forecast fields to be exchanged between the oceanic and atmospheric meshes.

The 27 km WRF domain is large enough to provide the surface forcing for the entire oceanic model. However, the oceanic mesh cannot provide a complete SST field for the atmospheric model. It is supplemented with the RTG_SST_HR product to provide complete coverage.

The synchronization points for data exchange in the coupled system are defined every half hour (1800 seconds), after the initialization. During the exchange, the air pressure, precipitation, air temperature, longwave and shortwave radiation fluxes and horizontal components of wind velocity are exchanged to the ROMS model. In the same instances, the SST is transferred from the ocean to the atmospheric model. The time steps are selected according to the stability conditions of each model.

2.4 Verification data

Data of hurricane Matthew are obtained from the Atlantic HURricane DATabase (HURDAT2). This database is a result of a post-storm analysis done by the National Hurricane Center (NHC) for each tropical cyclone in its area of responsibility Landsea *et al.* (2015). From this database, the verification data for the minimum center pressure, maximum sustained wind and best track are obtained.

To determine the track for each simulation, the submodule Cysearch, from the Detection, Report and Evaluation Module Sierra-Lorenzo *et al.* (2016) is used. This submodule allows the detection of the cyclonic vortex in the outputs of the WRF model, using the pressure field and wind intensity at the surface. Using this method, the center position (latitude, longitude), maximum winds and minimum center pressure at each forecast output are obtained.

As reference data in the precipitation analysis, values obtained from the CPC MORPHing technique (CMORPH) are used Joyce *et al.* (2004). This technique uses precipitation estimates that have been derived from low orbiter satellite microwave observations exclusively, and whose features are transported via spatial propagation information that is obtained entirely from geostationary satellite IR data.

Also, the modified method for Object-Based Diagnostic Evaluation (MODEMod) Rodríguez-Genó *et al.* (2016) is used to perform a spatial evaluation of the forecast precipitation field with respect to the reference (CMORPH) field. The method recognizes the precipitation areas as result of convolution and thresholding processes, which allowed grouping the most significant areas and filtering the weaker features that were of no interest to the user. A fuzzy logic algorithm is used in order of merge objects of the same field, and match similar objects of different fields. With this method, the Critical Success Index (CSI) is calculated, that mathematically is given by:

$$CSI = \frac{N_m}{N_m + N_o + N_p} \quad (1)$$

Where N_m is the number of selected pairs of objects (success), N_o is the number of objects detected in the reference field but not in the forecast (failure) and N_p is the number of objects detected in the forecast field but not in the reference (false alarms).

For SST verification, data derived from images of the geostationary satellite (GOES) are used. The SST values are calculated using a regression method and

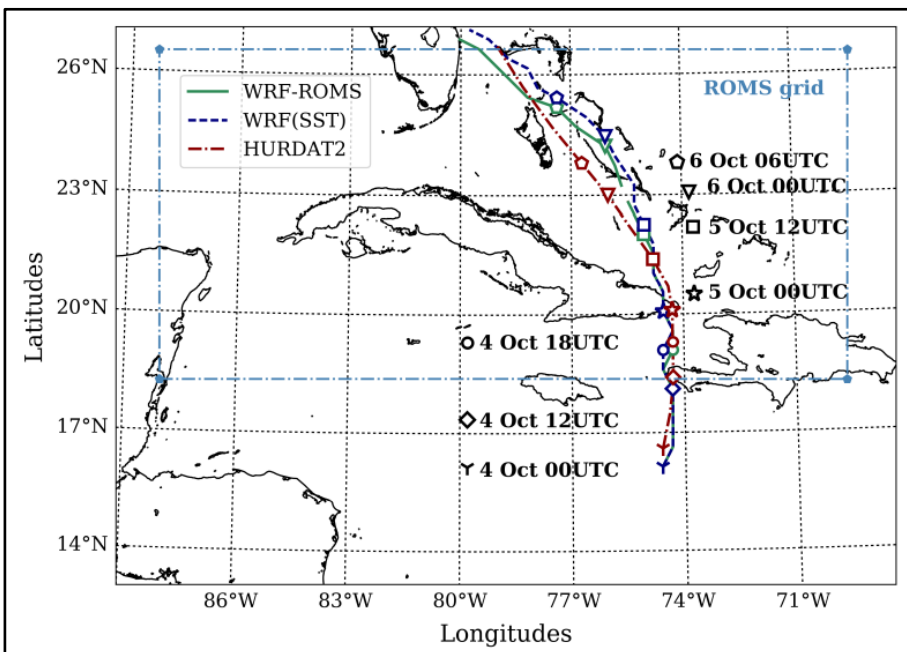
distributed in a rectangular mesh of 6 km of resolution. Over the land or where cloud cover prohibits the SST calculation, a mask is applied during verification. This data is available with a temporal resolution of 1 hour Maturi *et al.* (2008).

To postprocess the data, we created several scripts in the python language Oliphant (2007), Millman e Aivazis (2011). The packages Numpy Van Der Walt *et al.* (2011), Scipy Virtanen *et al.* (2020) and Matplotlib Hunter (2007) are used.

3 RESULTS AND DISCUSSION

This section is structured as follows: first, the SST simulations obtained for each experiment are briefly presented. After, a study of the coupling influence in the simulation accuracy of hurricane track, intensity and latent heat fluxes are performed. Finally, the effect of using a coupled system in the precipitation field and hurricane dry footprint are studied.

Image 2 - Comparison of track simulation for each experiment with best track



Source: created by the author (PROVEYER, 2021)

3.1 Hurricane movement and track

According to the best track, Hurricane Matthew was located at 16.6° N and 74.6° W on October 4th, 0000 UTC. The system kept a movement to the north until it made landfall on October 5th 0000 UTC in Guantánamo. After going out to the sea, its movement acquired a northwest component until October 7th. During this period, it maintained the category of major hurricane (category 3-4).

Figure 2 shows the comparison of tracks between both experiments, WRF (SST) and WRF-ROMS respect to the best track. During the first 12 hours of forecast, the tracks simulations are in good agreement. From that moment (October 4th at 1200 UTC), the hurricane is inside the section of the atmospheric domains in which the SST data is updated from the ROMS model.

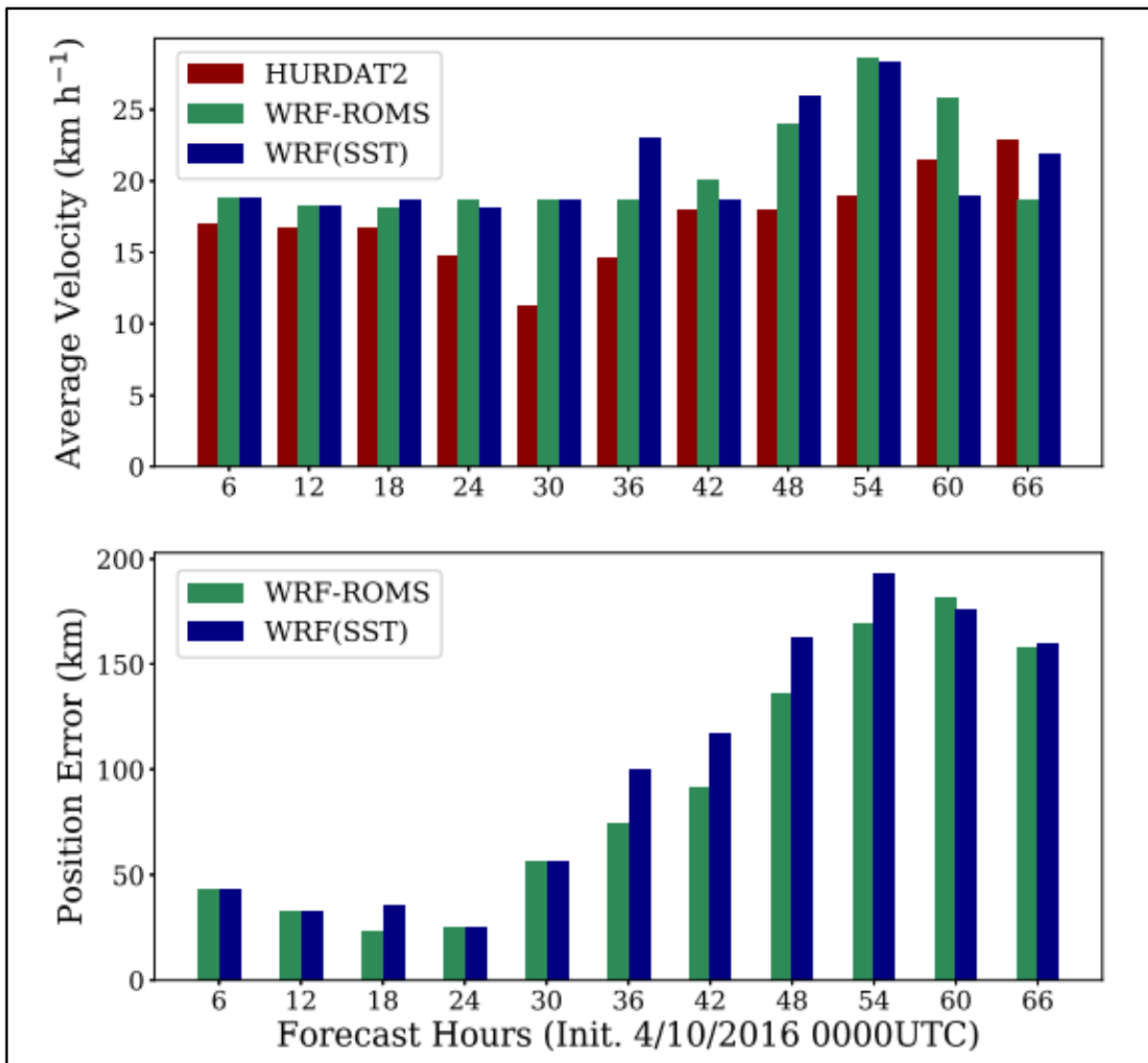
Position error (Figure 3, bottom panel) is computed as the difference between the NHC best track locations of the hurricane center at 6 hours' intervals and the storm center location in each experiment. The storm center position is determined by the Cysearch submodule for both experiments.

The hurricane made landfall on October 5th at 0000 UTC in both simulations, at 25.26 kilometers offset from the real position. Figure 3 (bottom panel) shows that the coupling positively influences the track simulations, decreasing the position error respect to the best track. The difference between the experiments increases with the forecast time. In general, the improvement that introduces the coupled system (WRF-ROMS) respect to WRF(SST) is greater as the forecast period increases; reducing the position error by 26.64 km at 48 hours of forecast (October 6th at 0000 UTC).

Figure 2 shows that after the first 24 forecast hours the hurricane moves ahead of the observed position in both experiments and its movement is faster in the following time frames. Figure 3 (top panel) shows that the mean hurricane velocity of translation in the simulations is greater than observations in most of the studied periods, reaching a maximum (approximately 9.56 kmh^{-1}) at the 54th-hour of the forecast.

Between the 24 and 36 forecast hours, the hurricane experiences a turn, characterized for a decrease of its velocity, which is shown in the HURDAT2 data. None of the numerical experiments shows a hurricane deceleration. However, in the WRF-ROMS simulation the average velocity remains constant while in the WRF (SST) experiment the velocity increases. In general, the best results are obtained using the coupled system in the track and movement simulations, as in previous studies Warner *et al.* (2010) Zambon *et al.* (2014).

Image 3 - Comparison of average velocity of hurricane translation and absolute error of hurricane position (km) respect to best track



Source: created by the author PROVEYER (2021)

3.2 Sea Surface Temperature Analysis

During the simulations, the cloudiness associated with the hurricane makes it difficult to determine the SST values in the area where the hurricane passes. For this reason, the data correspondent to October 1st at 0400 UTC is used to define the initial state of the sea thermal field before the hurricane pass. For the final state, after the hurricane pass, the SST field correspondent to October 8th at 0500 UTC is used. The pertinence of this approach is the great thermal inertia which characterize the oceans.

Figure 4 shows the SST behavior defined in two moments: before and after the hurricane passes. In both cases, with the coupled system the SST representation is more detailed.

Before the hurricane pass, using a dynamic SST (Figure 4 (a)), the SST values in the area where the hurricane will pass has a maximum of 29°C. While in the coupled system (Figure 4 (b)), the maximum SST values are approximately 31°C. The greater values using the coupling means a higher quantity of energy available to intensify the hurricane in this area. This amount of energy is consequent with a greater latent heat flux on October 4th at 1200 UTC (Figure 6, a) and higher wind velocities, respect to the uncoupled system.

After the hurricane, the SST values estimated using the coupled system are smaller than obtained using a dynamic SST. The sea surface cooling after a hurricane passes, known as coldprint, is better represented using the coupling (Figure 4 third column). In the WRF (SST) the SST variation is small, with values of approximately 1°C north of Cuba. However, using the WRF-ROMS the surface cooling is about 3°C. In the coupled system a better representation of the coldprint, principally in the areas along the hurricane track, is obtained.

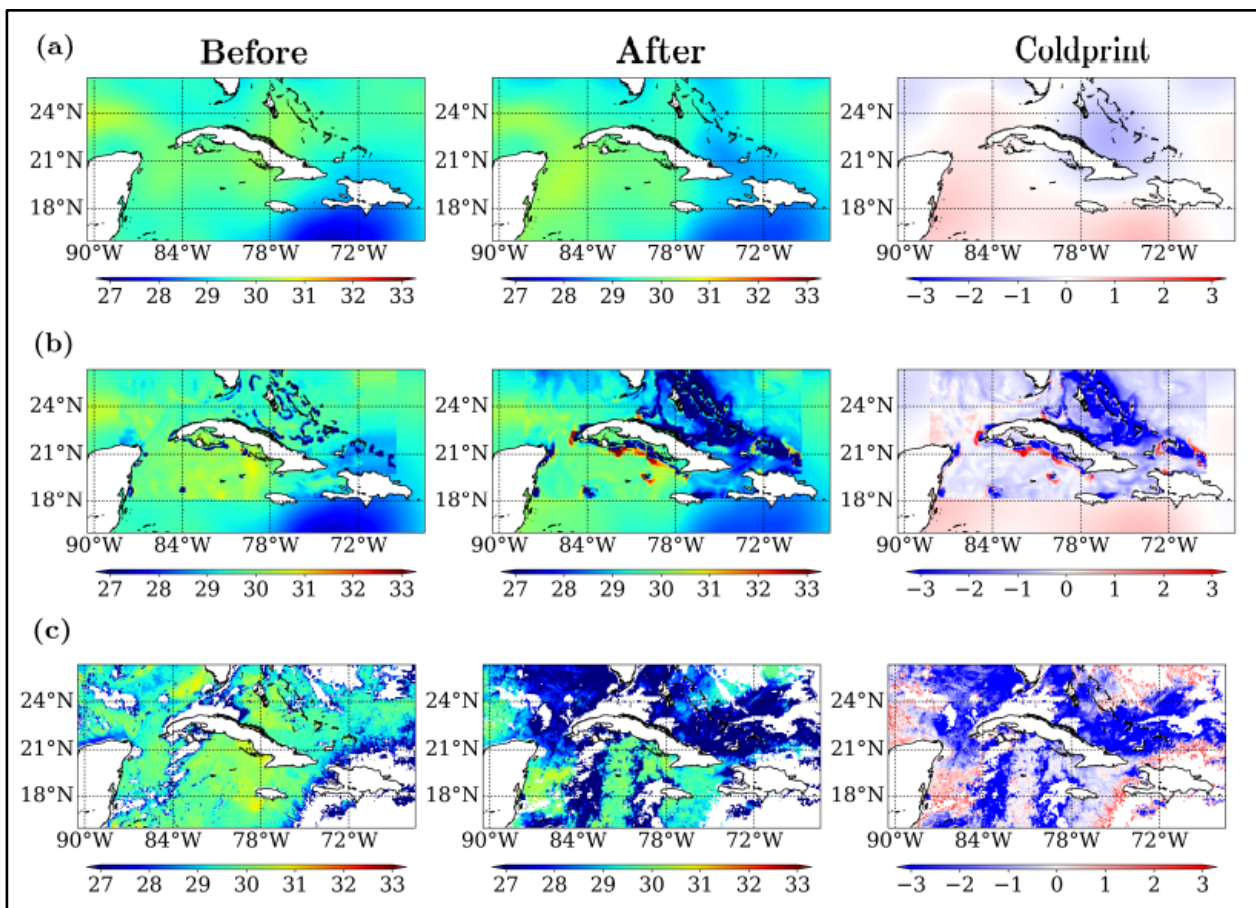
3.3 Hurricane intensity

In the intensity analysis, the highest errors are obtained. The analysis is based on the maximum wind speed and the minimum center pressure. The results are shown in Figure 5.

In Figure 5(a), the hurricane wind evolution predicted in both experiments do not agree well with the observed values, with very low values of maximum speed in all times studied. Using the coupled system did not significantly change results with respect to the first experiment.

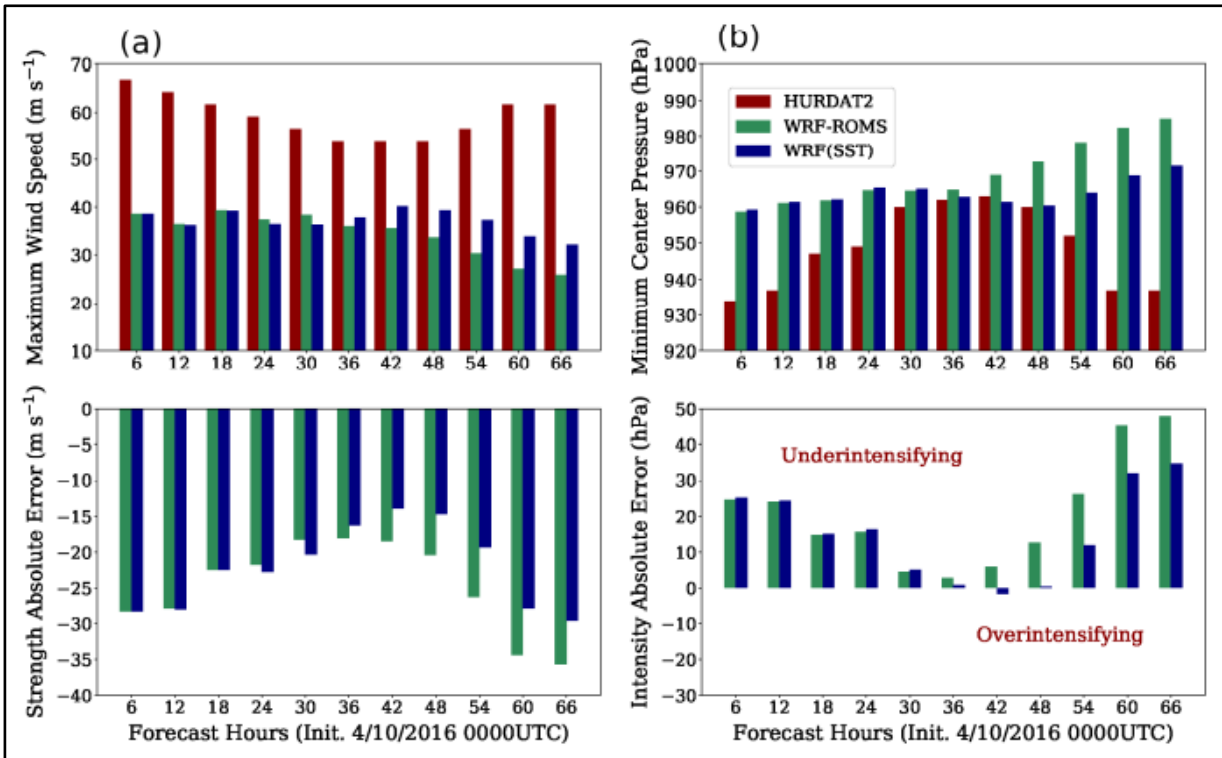
The more notable differences are observed in the last 24 forecast hours in the simulations (Figure 5(a) (bottom panel)). In both experiments the maximum wind velocity decreases from October 5th at 0000 UTC, decreasing less in the WRF (SST) experiment.

Image 4 - Oceanic thermal field (°C) before and after hurricane pass and the cooling of sea surface, for (a) WRF (SST), (b) WRF-ROMS and (c) GOES data.



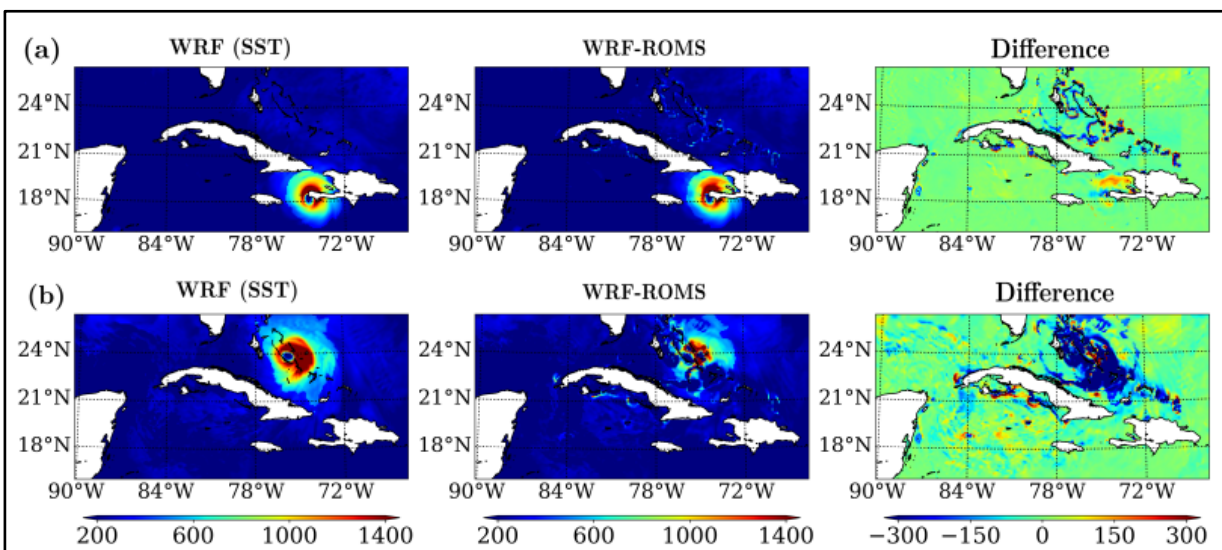
Source: created by the author (PROVEYER, 2021)

Image 5 - (a) Comparison of maximum wind speed (m/s) obtained on each experiment respect to HURDAT2 (superior panel) and absolute error (bottom panel) (b) Comparison of minimum center pressure (hPa) obtained on each experiment respect to HURDAT2 (top panel) and absolute error (bottom panel).



Source: created by the author (PROVEYER, 2021)

Image 6 - Surface latent heat fluxes (W m⁻²) for each experiment and the difference between them (coupled - uncoupled) (a) October 4th 1200 UTC (b) October 5th 2100 UTC



Source: created by the author (PROVEYER, 2021)

This could be due to the position error with respect to the HURDAT2 data is bigger, the hurricane is moving over shallow waters and its movement is faster (Figures 2 and 3). Using coupling, the available energy to strengthen is lower respect to the WRF (SST) due to lower SST values at north of Cuba (Figure 4).

The Figure 5(b) shows the comparison between the minimum center pressure calculated in each experiment, with the verification data from the HURDAT2. In general, in both experiments, during the simulations the hurricane intensity is under estimated (underintensified). In the coupled system, the pressure increases in the hurricane center towards the end; which corresponds with the decrease of the maximum wind velocity and therefore the weakening that experiments the hurricane in these times.

3.4 Latent heat fluxes

One of the most important energy sources in the tropics for hurricane development are the latent heat fluxes from the ocean. Figure 6 shows the surface latent heat fluxes simulations of each numerical experiment and its difference on October 4th at 1200 UTC and October 5th at 2100 UTC.

Figure 6(a) shows the surface flux simulations in both experiments on October 4th at 1200 UTC. In the coupled system the surface flux is more intense, fundamentally in the front of the hurricane, where the difference between the experiments is about $100\text{-}200\text{ Wm}^{-2}$. This difference in the simulations is related with higher values of SST in the coupled system at West of Haiti before the hurricane pass (Figure 4 first column). A greater amount of energy means greater wind speed values in the coupled system than the WRF(SST) experiment, as is shown in the next time frames (Figure 5(a)).

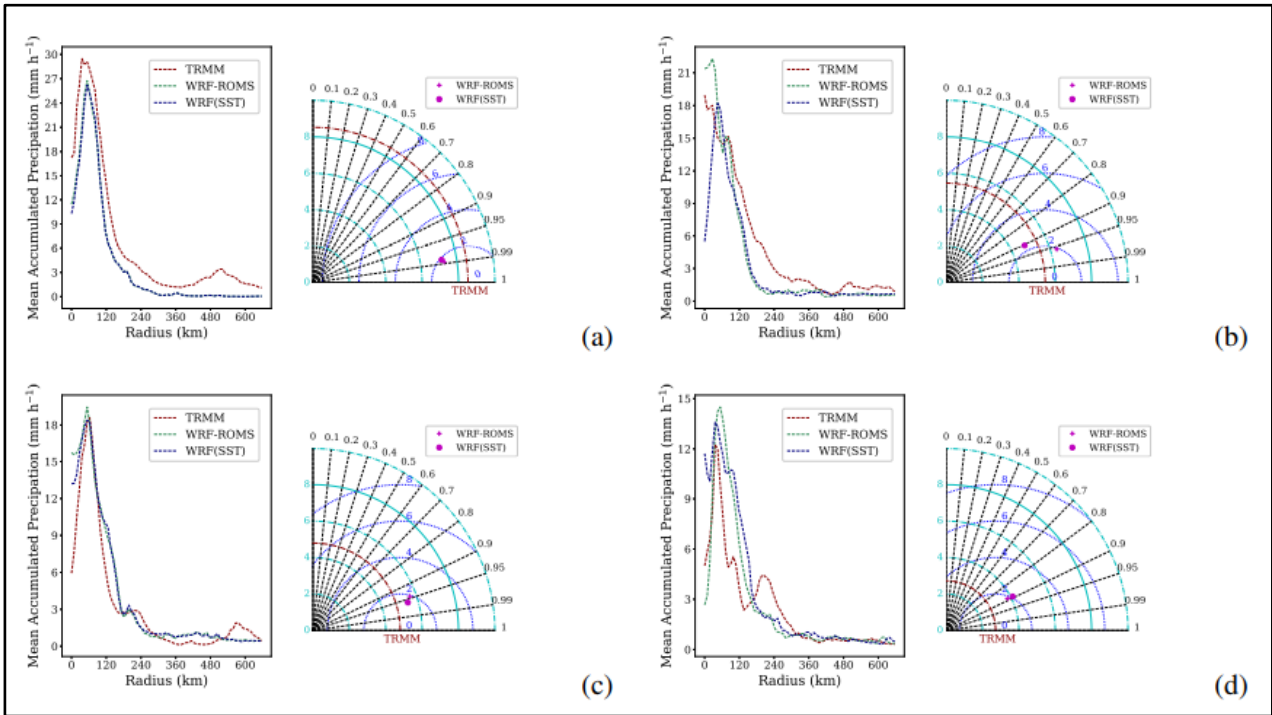
Figure 6(b) shows the latent heat flux at the surface on October 5th at 2100 UTC. In North of Cuba, where waters are shallower and the SST is lower, the flux

decreases in the simulations of the coupled system, which could explain the weakening of the winds and center pressure increase in the hurricane (Figure 5). In the numerical experiment without coupling this is not observed.

3.5 Precipitation and dry footprint analysis

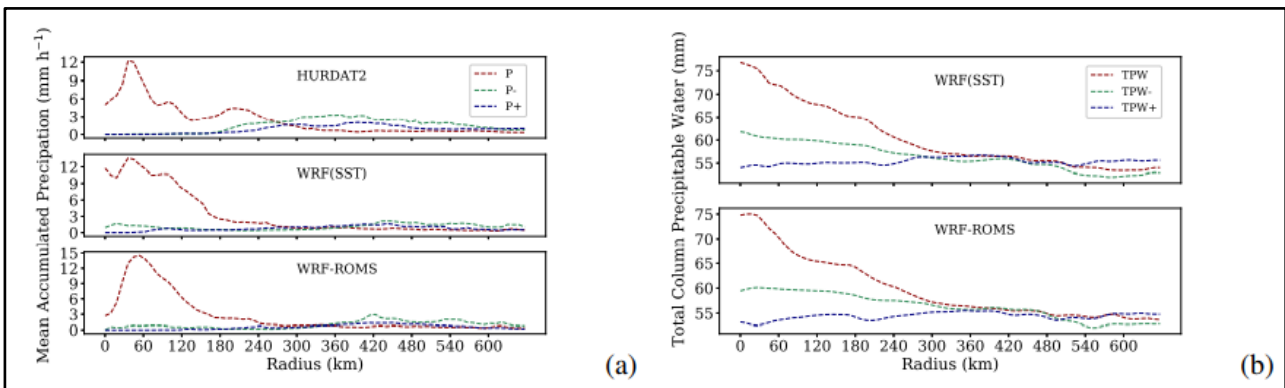
In this section are analyzed two variables: the accumulated precipitation and the total column precipitable water. The local values of both fields represent the mean values at a radius r_i respect to the hurricane center, where $0 < i < 73$ being $r_0 = 0\text{km}$ and $r_{73} = 657\text{km}$. Figure 7 shows the accumulated precipitation (in mmh^{-1}) at various times as obtained from TRMM data and both experiments initialized at October 4th. In the left panel are shown the behavior in function of the radial distance since the hurricane center. In the right one, are shown Taylor's diagrams with the aim of assessing the results obtained in each simulation through the analysis of the correlation coefficients (black), standard deviation (cyan) and centered root-mean-square differences (blue). The red circle represents the TRMM data (verification) standard deviation. The biggest differences in the results are observed in the first 120 km, where the area of significant convection is located in the hurricane (between 40-100 km according to Smith (2006)). In both experiments, the results are good, with correlation coefficients near or greater than 0.9 in the first 36 hours of simulation with centered root-mean-square differences less than 3. The coupled system tends to further overestimate the accumulated precipitation. However, the radial profiles are closer to the verification data with higher values of the correlation coefficient in the first 24 hours of simulation.

Image 7 - Comparison of mean accumulated precipitation (mmh^{-1}) radial behavior in both experiments respect to TRMM data and Taylor diagrams showing correlation coefficients (black), standard deviation (cyan) and centered root-mean-square differences (blue). a) October 4th 0600 UTC, b) October 4th 1800 UTC, c) October 5th 0000 UTC, d) October 5th 1200 UTC



Source: created by the author (PROVEYER, 2021)

Image 8 - Dry footprint analysis a) Comparison of mean accumulated precipitation (mmh^{-1}) at October 5th 1200 UTC and 24 hours before (P-) and after (P+) hurricane pass in that position. b) Comparison of total column precipitable water (mm) at October 5th 1200 UTC and 24 hours before (TPW-) and after (TPW+) hurricane pass in that position



Source: created by the author (PROVEYER, 2021)

The differences between the statistical parameters in the Taylor diagrams are not significant in the studied times, except on October 4th at 1800 UTC (Figure 7(b)), where the obtained profile in the coupled system is more accurate with a correlation coefficient of 0.9577 and in the uncoupled model is 0.9051.

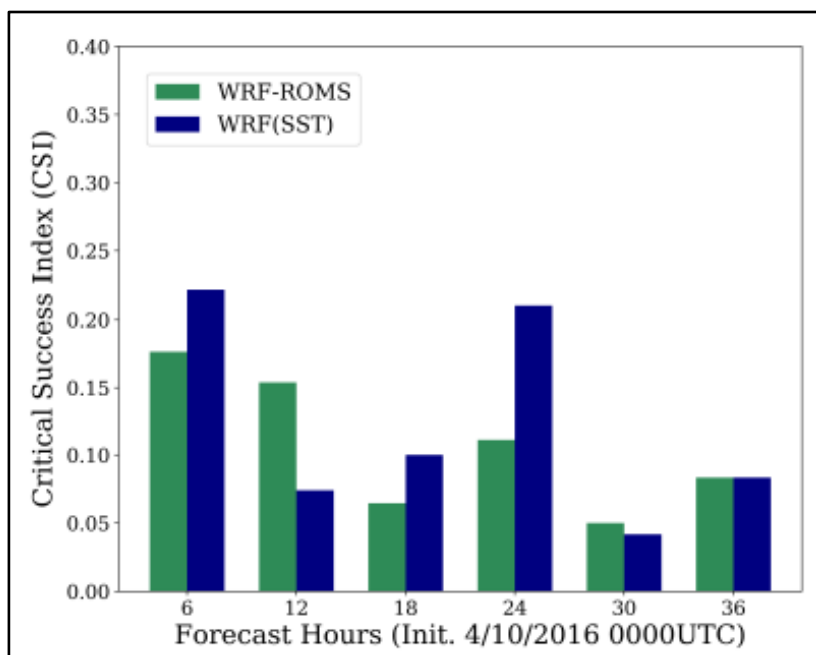
After 36 hours of simulation in both experiments, the errors of the accumulated precipitation profiles increase as a result of higher errors in the track simulations respect to the real position (Figure 3). Using the coupling, the profile errors are higher due to the weakening of the hurricane in that experiment, as well as its accelerated movement respect to the mean velocity calculated from HURDAT2 data.

Figure 8 shows the behavior of the accumulated precipitation: a) and the total column precipitable water (TPW), b) versus radius respect to the hurricane center position on October 5th at 1200 UTC and the behavior of these fields 24 hours before and after the hurricane pass. According to the American Meteorological Society Glossary Glickman (2000), the total column precipitable water (TPW) contained in a layer bounded by pressures p_1 and p_2 is given by:

$$TPW = \frac{1}{\rho g} \int_{p_1}^{p_2} x(p) dp \quad (2)$$

Where $x(p)$ is the mixing ratio at the pressure level p , ρ is water density and g is the gravity acceleration. As observed in Figure 8 (b) the TPW increases rapidly near to the hurricane center, where the quick ascent of the wind induces supersaturation Makarieva *et al.* (2017). This area coincides with the area of significant convection.

Image 9 - Critical Success Index obtained for each experiment in the spatial analysis of the accumulated precipitation field using the MODEMod_v1 software



Source: created by the author (PROVEYER, 2021)

According to Makarieva *et al.* (2017), in greater radius, the TPW is slightly higher than the existing quantity in the absence of a hurricane. This could reflect the fact that the wind velocities are developed preferentially when and where the amount of water vapor is higher than usual. This is supported by the results showing that the TPW 24 hours before is greater than 24 hours after the hurricane pass (Figure 8 (b)).

In the studied area, the greater TPW values before the hurricane pass indicate that the atmospheric moisture is expended faster than it is responsive for evaporation. This could show that hurricane is an open system that consumes preexisting vapor in the atmosphere during its movement. This mechanism that makes it self-sustained inside a radius of 700 km is defined as the dry footprint area, theoretically inside a radius of 500-600 km respect to the hurricane center Makarieva *et al.* (2017).

Figure 9 shows the CSI values obtained with the MODEMod software. Due to the overestimation of the accumulated precipitation values in both experiments

with respect to the verification, more objects identified during the forecast are false alarms. This is one of the main reason for small CSI values obtained in both simulations. Using the coupled system, the overestimation is greater (Figure 7) and the CSI values are less than the uncoupled experiment at 6, 18 and 24 forecast hours. The difference in CSI values between both experiments is maximum on October 5th at 0000 UTC (0.0994).

4 CONCLUSIONS

In this investigation, the coupled oceanic-atmosphere components of COAWST Modeling System are used as part of SisPI. Results shows a more detailed representation of the oceanic-atmosphere interaction during the hurricane Matthew.

The analysis and comparison of the coupled and uncoupled numerical experiments demonstrated the influence of the SST on the behavior of the atmospheric variables and therefore, in the atmospheric studied processes.

Better results in average velocity and position are obtained using the coupled system, with an improvement of the best track between 20-60 km with respect to the uncoupled system. Also, the SST has a strong influence in the latent heat flux simulations, associated with changes in hurricane intensity.

Concerning to the hurricane intensity, the wind speed forecast has high relative errors (greater than 10%) compared to HURDAT2 verification data. These errors in the intensity simulations can be due to the grid resolution used, using a higher resolution can improve the simulations. The use of a moving nest may be investigated for increased fidelity in the wind forecast.

In the analysis of the precipitation field, the coupled system tends to further overestimate the accumulated precipitation. However, the radial profiles are closer to the verification data with higher values of the correlation coefficient than the uncoupled system, in the first 24 hours of simulation.

Besides, the dry footprint is well represented and the analysis shows that a hurricane acts like an open and self-sustained system that depends on the atmospheric moisture it consumes during its movement.

REFERENCES

BALLESTER, M., RUBIERA, J. (2016). **Temporada ciclónica de 2016 en el atlántico norte.**

Available on:

<https://www.insmet.cu/asp/genesis.asp?TB0=PLANTILLAS&TB1=TEMPORADA&TB2=/Temporadas/temporada2016.html>. Accessed on: Mar. 2 2021.

BENDER, M. A., GINIS, I. (2000). Real-case simulations of hurricane–ocean interaction using a high-resolution coupled model: Effects on hurricane intensity. **Monthly Weather Review**, 128(4), 917–946.

BOOIJ, N., HOLTHUIJSEN, L., RIS, R. (1997). The "swan" wave model for shallow water. In: **Coastal Engineering** 1996, pp. 668–676.

EGBERT, G. D., EROFEEVA, S. Y. (2002). Efficient inverse modeling of barotropic ocean tides. **Journal of Atmospheric and Oceanic technology**, 19(2), 183–204.

GEMMILL, W., KATZ, B., LI, X. (2007). Daily real-time, global sea surface temperature—high-resolution analysis: Rtg_sst_hr. ncep. **Relatório Técnico**, EMC Tech. Rep. 260, 39 pp. Available on: <http://polar.ncep.noaa.gov>. Accessed on: Jan. 12 2020

GEYER, W., SHERWOOD, C. R., KEEN, T. (2007). Community sediment transport model. **Relatório Técnico**, WOODS HOLE OCEANOGRAPHIC INSTITUTION MA.

GLICKMAN, T. (2000). **Glossary of Meteorology**. American Meteorological Society. Available on: http://glossary.ametsoc.org/wiki/Precipitable_water. Accessed on: Mar. 2 2021.

GRELL, G. A., FREITAS, S. R. (2014). A scale and aerosol aware stochastic convective parameterization for weather and air quality modeling. **Atmospheric Chemistry and Physics**, 14(10), 5233–5250.

HEGERMILLER, C. A.; *et al.* (2019). Wave–current interaction between hurricane matthew wave fields and the gulf stream. **Journal of Physical Oceanography**, 49(11), 2883–2900.

HUNTER, J. D. (2007). Matplotlib: A 2d graphics environment. **IEEE Annals of the History of Computing**, 9(03), 90–95.

JONES, P. W. (1999). First-and second-order conservative remapping schemes for grids in spherical coordinates. **Monthly Weather Review**, 127(9), 2204–2210.

JOYCE, R. J.; *et al.* (2004). Cmorph: A method that produces global precipitation estimates from passive microwave and infrared data at high spatial and temporal resolution. **Journal of hydrometeorology**, 5(3), 487–503.

LANDSEA, C., FRANKLIN, J., BEVEN, J. (2015). The revised atlantic hurricane database. **Relatório Técnico**, National Hurricane Center.

LARSON, J. W.; *et al.* (2001). The model coupling toolkit. In: **International Conference on Computational Science**, Springer, pp. 185–194.

LIM, J. O. J., HONG, S., DUDHIA, J. (2004). The wrf single-moment-microphysics scheme and its evaluation of the simulation of mesoscale convective systems. In: **20th Conference on Weather Analysis and Forecasting/16th Conference on Numerical Weather Prediction**, Seattle, pp. 1–15.

MAKARIEVA, A. M.; *et al.* (2017). Fuel for cyclones: The water vapor budget of a hurricane as dependent on its movement. **Atmospheric Research**, 193, 216–230.

MATURI, E.; *et al.* (2008). Noaa's sea surface temperature products from operational geostationary satellites. **Bulletin of the American Meteorological Society**, 89(12), 1877 – 1888. Available on:
https://journals.ametsoc.org/view/journals/bams/89/12/2008bams2528_1.xml. Accessed on: Feb. 3 2020

MICHALAKES, J.; *et al.* (2005). The weather research and forecast model: software architecture and performance. In: **Use of high performance computing in meteorology**, World Scientific, pp. 156–168.

MILLMAN, K. J., AIVAZIS, M. (2011). Python for scientists and engineers. **Computing in Science & Engineering**, 13(2), 9–12.

MITRANI-ARENAL, I.; *et al.* (2019). Coastal flood forecast in cuba, due to hurricanes, using a combination of numerical models. **Revista Cubana de Meteorología**, 25(2), 121–138.

OLIPHANT, T. E. (2007). Python for scientific computing. **Computing in Science & Engineering**, 9(3), 10–20.

RODRÍGUEZ-GENÓ, C. F., SIERRA-LORENZO, M., FERRER-HERNÁNDEZ, A. L. (2016). Modificación e implementación del método de evaluación espacial modemod para su uso operativo en cuba. **Ciencias de la Tierra y el Espacio**, 17(1), 18–31.

SHCHEPETKIN, A. F., MCWILLIAMS, J. C. (2005). The regional oceanic modeling system (roms): a split-explicit, free-surface, topography-following-coordinate oceanic model. **Ocean modelling**, 9(4), 347–404.

SIERRA-LORENZO, M.; *et al.* (2014). Sistema automático de predicción a mesoescala de cuatro ciclos diarios. **Relatório Técnico**, Instituto de Meteorología de Cuba.

SIERRA-LORENZO, M.; *et al.* (2016). Herramientas de detección, reporte y evaluación para salidas de modelos de pronóstico numérico desarrollado en cuba. **Revista Cubana de Meteorología**, 22(2), 150–163.

SIERRA-LORENZO, M.; *et al.* (2017). Estudios de sensibilidad del sispi a cambios de la pbl, la cantidad de niveles verticales y, las parametrizaciones de microfísica y cúmulos, a muy alta resolución. **Relatório Técnico**, Instituto de Meteorología de Cuba.

SMITH, R. K. (2006). **Lectures on tropical cyclones**.

VAN DER WALT, S., COLBERT, S. C., VAROQUAUX, G. (2011). The numpy array: a structure for efficient numerical computation. **Computing in science & engineering**, 13(2), 22–30.

VÁZQUEZ-PROVEYER, L.; *et al.* (2017). Estudios de sensibilidad en la interacción numérica océano-atmósfera. **Ciencias de la Tierra y el Espacio**, 18(1), 59–70.

VIRTANEN, P.; *et al.* (2020). SciPy 1.0: Fundamental Algorithms for Scientific Computing in Python. **Nature Methods**, 17, 261–272.

WALLCRAFT, A.; *et al.* (2003). Hybrid coordinate ocean model (hycom) version 2.1. user's guide. **Relatório Técnico**, Naval Research Lab Stennis Detachment Stennis Space Center MS.

WARNER, J.; *et al.* (2019). **A coupled ocean atmosphere wave sediment transport numerical modeling system (coawst)**: Us geological survey software. US Geological Survey: Reston, VA, USA.

WARNER, J. C., ARMSTRONG, B., HE, R., ZAMBON, J. B. (2010). Development of a coupled ocean–atmosphere–wave–sediment transport (coawst) modeling system. **Ocean modelling**, 35(3), 230–244.

WEATHERALL, P.; *et al.* (2015). A new digital bathymetric model of the world's oceans. **Earth and Space Science**, 2(8), 331–345.

WESSEL, P., SMITH, W. H. (1996). A global, self-consistent, hierarchical, high-resolution shoreline database. **Journal of Geophysical Research: Solid Earth**, 101(B4), 8741–8743.

ZAMBON, J. B., HE, R., WARNER, J. C. (2014). Investigation of hurricane ivan using the coupled ocean–atmosphere–wave–sediment transport (coawst) model. **Ocean Dynamics**, 64(11), 1535–1554.

Authorship contributions

1 – Liset Vázquez Proveyer

BSc. on Meteorology, Meteorology Specialist in Center for Atmospheric Physics, Cuban Institute of Meteorology, Havana Cuba

<https://orcid.org/0000-0002-9291-3629> - lvproveyer@gmail.com

Contribution: Methodology, Investigation, Visualization, Writing - Review & Editing

2 – Maibys Sierra Lorenzo

PhD. on Mathematics Sciences, Meteorology Specialist in Center for Atmospheric Physics, Cuban Institute of Meteorology, Havana, Cuba

<https://orcid.org/0000-0003-4838-1474> - maibys.lorenzo@insmet.cu

Contribution: Conceptualization, Methodology, Investigation, Writing – Original Draft

3 – Roberto Carlos Cruz Rodríguez

MSc. on Mathematics Sciences, PhD Student in Institute of Atmospheric Sciences and Climate Change, National Autonomous University of Mexico (UNAM), DF, Mexico

<https://orcid.org/0000-0001-8783-8014> - roberto.cruz.rdg@gmail.com

Contribution Validation, Writing - Review & Editing

4 – John C Warner

PhD. on Civil and Environmental Engineering, Oceanographer in US Geological Survey, Coastal and Marine Hazards and Resources Program, Woods Hole Coastal and Marine Science Center, Woods Hole, MA 02543, United States

<https://orcid.org/0000-0002-3734-8903> - jcwarner@usgs.gov

Contribution Conceptualization, Software, Writing - Review & Editing

How to quote this article

PROVEYER, L. V.; LORENZO, M. S.; RODRÍGUEZ, R. C. C.; WARNER, J. C. Impacts of the ocean-atmosphere coupling into the very short range prediction system, during the impact of Hurricane Matthew on Cuba. **Ciência e Natura**, Santa Maria, v. 44, e3, 2022. Available in: <https://doi.org/10.5902/2179460X66169>.